Ordered hydrogen overlayers on metal surfaces

J. -P. Muscat
Institut de Physique Théorique, Université de Lausanne, CH 1015 Lausanne, Switzerland
(Received 21 October 1985)

The formation of ordered hydrogen overlayers on the close-packed surfaces of fcc and hcp metals is investigated. We consider hydrogen adsorption on seven metals (Ti, Co, Ni, Cu, Ru, Rh, and Pd) and we assume that the hydrogen atoms are adsorbed in the threefold hollow sites. We examine the question of site preference between the fcc and hcp sites and find substantial differences in binding energies between the two sites for all but one of these metals (Ni). The interaction energies between adatoms are then calculated. It is found that the multiple-adatom interactions can, to a high degree of accuracy, be written as the sum of the relevant pair interactions. Short-range interactions involving adatoms located at nearest-neighbor sites are found to be extremely repulsive indicating that nearest-neighbor exclusion is a prerequisite in the choice of the ordered overlayer. Long-range interactions (up to sixth neighbor) are found to be non-negligible and play an important role in determining which ordered overlayer is most likely to be formed. Information regarding the stability of different structures was obtained from considerations of the ground-state energies of a number of plausible ordered structures. The results for each metal are analyzed and compared to experiment, whenever possible. Excellent agreement with experiment is found for H/Ni(111) but a less satisfactory state of affairs is recorded for H/Pd(111).

I. INTRODUCTION

The adsorption of hydrogen atoms on transition- and noble-metal surfaces has recently been the object of an ever-increasing number of studies.[1] The experimental data on such systems is considerable, ranging from measurements of such quantities as binding energies[2] and changes in work function, to the characterization of the electronic structure of the chemisorbed system[3] and also to the determination of the geometry of the chemisorbed layer.[4]

These experimental studies have been supplemented by calculational schemes designed to throw some light upon the nature of the hydrogen-metal chemical bond. Amongst the most commonly used techniques is the so-called layer-type calculation, in which a layer of adatoms is made to interact with a substrate film consisting of a small number of metal layers. The two-dimensional band structure of the film is then determined and in some cases the total energy of the chemisorbed system is also calculated. Some of the more commonly used band structure schemes are the linearized augmented plane-wave (LAPW) method[5,6] and the pseudopotential method.[7] Another school of thought employs the cluster concept in which one adatom is made to interact with a small number of metal atoms. The energy spectrum of the cluster is then derived, as well as such quantities as binding energies, vibration frequencies, and equilibrium distances.[8] Apart from the very large computational effort which both these approaches require, further limitations are encountered in the strong degree of idealization which is present in both methods. For example, the layer-type calculations only treat the high coverage limit of chemisorption. The main limitation of the cluster concept concerns its isolated nature. Not only are the long-range effects of the hydrogen-metal bond neglected, there is the further introduction of unwanted surface effects at the extremity of the cluster where ideally more metal atoms ought to be.

Another approach to the subject is to consider the more natural problem of a single adatom interacting with a semi-infinite host which is represented by an effective medium[9] which in its simplest form takes on the appearance of a homogeneous electron gas. Effects due to the nonuniformity of the substrate electron density are calculated in perturbation theory within the region close to the adatom. Outside this region, the metal potential is treated exactly, but the adatom is now treated as the perturbation. This scheme has been used to obtain potential energy curves for various hydrogen-metal systems.[9]

None of the above-mentioned models treats the problem of adatom-adatom interactions explicitly. Clearly, these interactions are present in the layer-type calculations, but no information as to their relative strength can be obtained. A knowledge of these quantities is of paramount importance in the description of the order-disorder transitions which are known to exist for certain hydrogen—transition-metal systems.[10]

The interaction between adatoms on a substrate surface is made up of many contributions. There is, in the first instance, the direct interaction arising from the overlap between the orbitals of the different adatoms. This interaction is of extremely short range, being significant for adatom-adatom separations of the order of molecular bond lengths. Another contribution to the interaction is the van der Waal's attraction between atoms which represents the dominant contribution for rare-gas physisorption on surfaces, but which is negligible in the case of chemisorbed species on metal surfaces. There is also an electrostatic interaction between dipoles which arise when adsorbing atoms gain from (or lose to) the substrate a sub-

stantial amount of charge, as is the case in alkali adsorption on metals. However, in hydrogen chemisorption, the transfer of charge between adatom and substrate is small, resulting in a negligible electrostatic contribution to the interaction. The most important contribution to the interaction between adatoms is an indirect interaction which arises from the mutual coupling of the adatom valence shells through the substrate valence band. Theoretical studies of this problem exist, most of which use a molecular orbital or Anderson model description as the starting point.[11–16]

We shall, in the following, be mainly interested in those chemisorption systems in which the substrate surface is the close-packed surface of fcc or hcp transition metals. Dissociative chemisorption of the hydrogen molecule occurs on all these transition metals.[17] Hydrogen-induced states have been observed in angle-resolved ultraviolet photoemission spectroscopy (ARUPS) experiments for most of these metals [Ti,[18] Co,[19] Ni,[3] Ru,[20] Pd,[3,21] and Pt (Ref. 3)]. Further, although there is an activation energy barrier for dissociation on Cu(111), a similar hydrogen-induced structure also exists for the adsorption of atomic hydrogen on Cu(111).[22] Ordered hydrogen overlayers have been observed on Ni and Pd (111) surfaces. For H/Ni(111), low-energy electron diffraction (LEED) experiments[23,24] have shown the presence of a (2×2) structure which is attributed to the formation of a honeycomb overlayer with the hydrogen atoms occupying both types of threefold hollow sites [see Fig. 1(d)]. The H–Ni separation was also derived and found to be equal to 1.84 Å. The (2×2) structure was observed over a fairly wide range of hydrogen coverages, centered around $\Theta=\frac{1}{2}$, and the transition temperature was given as $T=270$ K. For H/Pd(111), LEED data[25] shows the presence of two $(\sqrt{3}\times\sqrt{3})$ structures, centered at hydrogen coverages of $\theta=\frac{1}{3}$ and $\frac{2}{3}$. The transition temperatures for the two phases are, respectively, 90 and 105 K. These two structures are attributed to the formation of the ordered overlayers depicted in Figs. 1(c) and 1(f) where only one type of threefold hollow site is occupied. For the close-packed surfaces of rhodium,[26] ruthenium,[27] and platinum,[28] LEED experiments show no extra LEED spots, which may be interpreted in terms of a (1×1) hydrogen overlayer or in terms of a disordered hydrogen layer.

It appears that for these substrate surfaces, the most probable adsorption sites for the hydrogen adatoms are the threefold hollow sites. For H/Ni(111), a comparison between the theoretical and experimental intensity-versus-voltage curves obtained in the LEED measurements showed that both types of hollow sites were equally likely to be occupied.[24] Minimizations of the hydrogen-metal binding energy in various theoretical models[8,9] also tend to favor the threefold hollow sites at the expense of bridge or atop sites, although a great deal of mobility of the hydrogen adatoms on the surface has been hinted at.[29,30]

If one assumes that the hydrogen atoms occupy the threefold hollow sites, then the network of sites is a honeycomb lattice. However, since there are two types of site (the fcc and the hcp sites) and since *a priori* one type of site may be considerably more favorable to the hydrogen atoms than the other, the honeycomb lattice should be decomposed into two interpenetrating triangular lattices.

The most probable ordered structures on a honeycomb lattice are illustrated in Fig. 1. [Note that only the (7×7) and (2×2) structures of Figs. 1(b) and 1(d) require occupation of both types of site.] We have assumed that the nearest-neighbor interaction is infinitely repulsive, on account of the very short H–H distance encountered in such cases ($d_1=a/\sqrt{6}$ for fcc crystals or $d_1=a/\sqrt{3}$ for hcp crystals in terms of the lattice parameters of these crystals, giving distances around 1.5 Å for most metals). Calculations of pair interactions between hydrogen adatoms indicate very repulsive interactions at such distances.[31,32] In order to determine which ordered overlayers are most likely to be formed on the substrate surface, one needs to know the various interactions between the adatoms as well as the difference in binding energy between the different sites on the surface. In fact, the lattice-gas Hamiltonian is simply given by

$$H-\mu N=-(\epsilon+\mu)\sum_i n_i-\sum_{i\neq j} v_{ij}n_in_j-\sum_{i\neq j\neq k} v_{ijk}n_in_jn_k-\Delta\epsilon\sum_i{}' n_i\ . \tag{1}$$

μ is the chemical potential, N the number of occupied sites in the lattice. $n_i=0$ or 1 according to whether site i is empty or occupied. ϵ and $\epsilon+\Delta\epsilon$ are the hydrogen binding energies to the two different types of site. The summations are over all lattice sites except for the last summation which is over only half the sites. v_{ij} is the pair interaction energy between the hydrogen adatoms at site i and j. v_{ijk} is a three-body interaction term which accounts for the nonpairwise interactions linking atoms i, j, and k—in other words the energy corresponding to three occupied at sites i, j, and k is given by $-v_{ij}-v_{jk}-v_{ki}-v_{ijk}$. Higher-order terms may also be included in the Hamiltonian, although one would expect the higher-order terms to be vanishingly small.

We present in the following a method for calculating $\Delta\epsilon$ and the various interaction energies. We have illustrated in Fig. 2 the two types of threefold hollow sites (fcc and hcp), the pair interactions p_i between two ith-nearest-neighbor sites ($i=1$–6), the triangular interactions t_j linking three adatoms located at the vertices of the jth smallest equilateral triangular ($j=1,2,3$), and the hexagonal interactions h_k linking six adatoms at the vertices of the kth smallest regular hexagon ($k=1$–4). It is clearly seen that t_1, t_2, and t_3 are associated with the

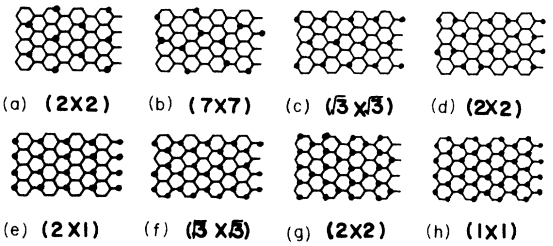

FIG. 1. Possible ordered overlayers on honeycomb lattice.

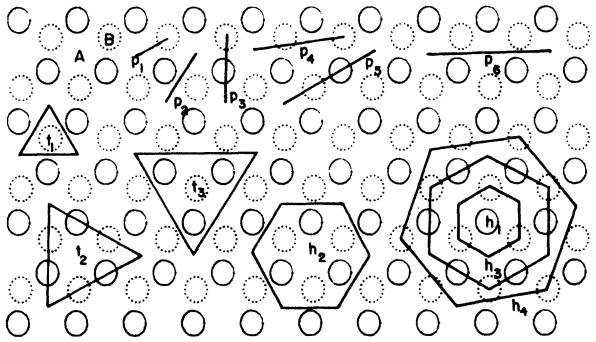

FIG. 2. fcc (A) and hcp (B) sites; pair, triangular, and hexagonal interactions on close-packed surface of fcc and hcp metals. Solid circles represent surface atoms, dashed circles represent subsurface atoms.

(1×1), $(\sqrt{3}\times\sqrt{3})$, and $p(2\times2)$ structures of Figs. 1(h), 1(c), and 1(a), respectively; h_2, h_3, and h_4 are associated with the $(\sqrt{3}\times\sqrt{3})$, (2×2), and (7×7) structures of Figs. 1(f), 1(d), and 1(b), while a combination of h_2 and t_1 leads to a Kagomé arrangement associated with the $p(2\times2)$ structure of Fig. 1(g). h_1 is not associated with any of the ordered structures illustrated in Fig. 1, since we have imposed at the outset nearest-neighbor exclusion.

The method employed is an embedded cluster model, which has been presented in detail elsewhere.[33] Preliminary results for H on Ni(111) have already been published.[34] In addition to these results, we also present results for hydrogen adsorption on the close-packed surfaces of Ti, Co, Cu, Ru, Rh, and Pd. The formalism is briefly described in Sec. II, and the results and discussion follow in Sec. III.

II. FORMALISM

As discussed in the Introduction, the important quantities relating to order or disorder on the surface are the difference in binding energy between hydrogen atoms adsorbed in fcc or hcp hollow sites and the various interaction energies linking two or more adatoms. In order to calculate these quantities, we represent both the adatoms and the metal atoms by spherically symmetric potentials inscribed within muffin tins. For the metal atoms self-consistent bulk band structure potentials were chosen,[35] while for the hydrogen atoms the potential was parametrized in such a way that it produced a doubly occupied bound state just below the bottom of the sp band when immersed in bulk jellium, as observed in first-principles calculations for a H proton in jellium of density $r_s > 1.9$ a.u.[36] The potential outside the muffin tins is assumed to be constant except for a planar infinite discontinuity which represents the surface potential. It is then found that the change in the sum of one-electron energies upon moving the hydrogen adatom from the fcc to the hcp site is given by

$$\delta E^1 = -\frac{2}{\pi}\int_{-\infty}^{\epsilon_F}[\delta_A(E)-\delta_B(E)]dE\ , \tag{2}$$

where δ_A (δ_B) is the integrated change in density of states introduced by one hydrogen adatom occupying the fcc site (site A) or the hcp site (site B), i.e.,

$$\delta_s(E)=\frac{\pi}{2}-\arg\left[T_{s00,s00}-\sum_{i,j}T_{s00,ilm}\,(T^{-1})_{ilm,jl'm'}\times T_{jl'm',s00}\right], \tag{3}$$

where $s=A,B$. The summation is over all the metal sites in the cluster and their orbital and azimuthal quantum numbers l and m. The scattering matrix elements are given by

$$T_{ilm,jl'm'}=\frac{ie^{-i\delta_{i,l}}}{\sin\delta_{i,l}}\delta_{ij}\delta_{ll'}\delta_{mm'}+4\pi\sum_{l''m''}i^{l-l'-l''}I_{ll'l''}^{mm'm''}[h_{l''}(kR_{ij})Y_{l''m''}^*(R_{ij})-(-1)^{l+m}h_{l''}(kR_{ij}^+)Y_{l''m''}^*(R_{ij}^+)]\ , \tag{4}$$

where $\delta_{i,l}$ are the l-dependent phase shifts produced by the potential inside the muffin tin centered on site i, $\mathbf{R}_{ij}$ is the vector joining site i to site j and $\mathbf{R}_{ij}^+$ is the vector joining i to the image of j in the plane of the infinite barrier, h_l are the spherical Hankel functions, and $I_{ll'l''}^{mm'm''}$ are the Gaunt integrals.[37]

Clearly δE^1 represents only the change in the sum of one-electron energies as the hydrogen atom is moved from the fcc to the hcp site and not the difference in binding energy $\Delta\epsilon$ between the sites. One way to calculate $\Delta\epsilon$ is to use the effective-medium model[38] which basically tells us that $\Delta\epsilon$ is made up of the two terms

$$\Delta\epsilon=\delta E^1+\Delta E^0(\langle n_A\rangle)-\Delta E^0(\langle n_B\rangle)\ , \tag{5}$$

where

$$\Delta E^0(n)=\Delta E^{\rm hom}(n)-\alpha n \tag{6}$$

and $\Delta E^{\rm hom}(n)$ is the binding energy of the hydrogen impurities to a homogeneous electron gas of density n and αn is an electrostatic term with α, a constant, $\langle n_a\rangle$, $\langle n_B\rangle$ are the average charge densities taken over the hydrogen-induced electrostatic potential $\Delta\varphi$ at the fcc and hcp site, respectively, i.e.,

$$\langle n\rangle=\int_a\Delta\varphi(\mathbf{r})n(\mathbf{r})d\mathbf{r}\Big/\int_a\Delta\varphi(\mathbf{r})d\mathbf{r}\ , \tag{7}$$

where a is taken as a sphere of radius 2.5 a.u. and $n(\mathbf{r})$ is represented as a superposition of atomic charge densities

obtained from atomic tables.[39] $\Delta\varphi(\mathbf{r})$ is calculated with the assumption that the hydrogen-induced charge density is zero.

If more than one hydrogen adatom is present on the substrate surface, then the interaction energy between the adatoms is given by the following relation:

$$V^{(n)}=-\frac{2}{\pi}\int\left[\delta^{(n)}(E)-\sum_{r=1}^{n}\delta_r(E)\right]dE\ , \tag{8}$$

where δ_r is given by (2) for different positions $r=1,2,\ldots,n$ which one adatom occupies and $\delta^{(n)}$ is the corresponding quantity for the n interacting hydrogen atoms, i.e.,

$$\delta^{(n)}(E)=\frac{n\pi}{2}-\arg\{\det[X^{(n)}(E)]\}\ , \tag{9}$$

$X^{(n)}$ is an $(n\times n)$ matrix whose elements are given by

$$X^{(n)}_{pq}=T_{p00,q00}-\sum_{\substack{ijll'\\mm'}}[T_{p00,ilm}(T^{-1})_{ilm,jl'm'}T_{jl'm',q00}]\ , \tag{10}$$

and the sum is again over all metal sites in the cluster and their orbital and azimuthal quantum numbers. Clearly $V^{(n)}$ corresponds to the different p_i's for $n=2$, t_j's for $n=3$, and h_k's for $n=6$ (see Fig. 2).

The equation for $V^{(n)}$ is exact to first order in the change in charge density induced by an adatom at the sites of the others. The effects due to these changes in charge density have been discussed within the effective medium theory for hydrogen adsorption on the (100) faces of Ni and Pd.[40]

In order to calculate these quantities, one needs to specify the cluster of metal atoms. In the calculation of $\Delta\epsilon$ we have considered the following procedure of constructing the cluster. We have calculated the binding energies of an atom in an fcc site and then in an hcp site on the same cluster and subtracted. The cluster used is illustrated in Fig. 3 and comprises the three atoms closest to both hollow sites as well as the nearest neighbors to the atoms. The difficulty with this approach is that there is no symmetry at either of the two sites and consequently the cluster size is limited. Another approach one could use is to consider different clusters for each site and thus to calculate the binding energies separately. The clusters can be constructed shell by shell. One starts with the three atoms closest to the adsorption site; one then introduces the nearest neighbors, next-nearest neighbors, and so on. The advantage of this approach is that the symmetry of the adsite (symmetry 3) may be used to reduce the size of the matrix T considerably. The disadvantage of this approach is that the binding energy of the hydrogen atom to the two different sites is calculated using two different clusters, in which case, effects due to the different cluster configurations may be introduced.

In the calculation of the multiple adatom interactions, we have used the symmetry of the adatom ring as much as possible and constructed clusters accordingly. The 19-atom cluster illustrated in Fig. 4(a) was used to calculate

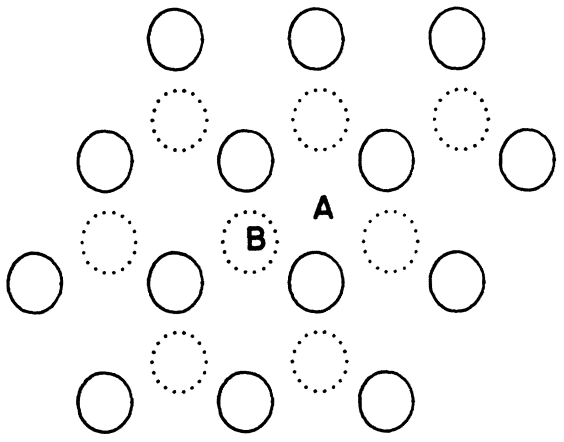

FIG. 3. Cluster used in calculation of hydrogen binding-energy difference between fcc and hcp sites. Solid circles represent surface atoms and dashed circles subsurface atoms.

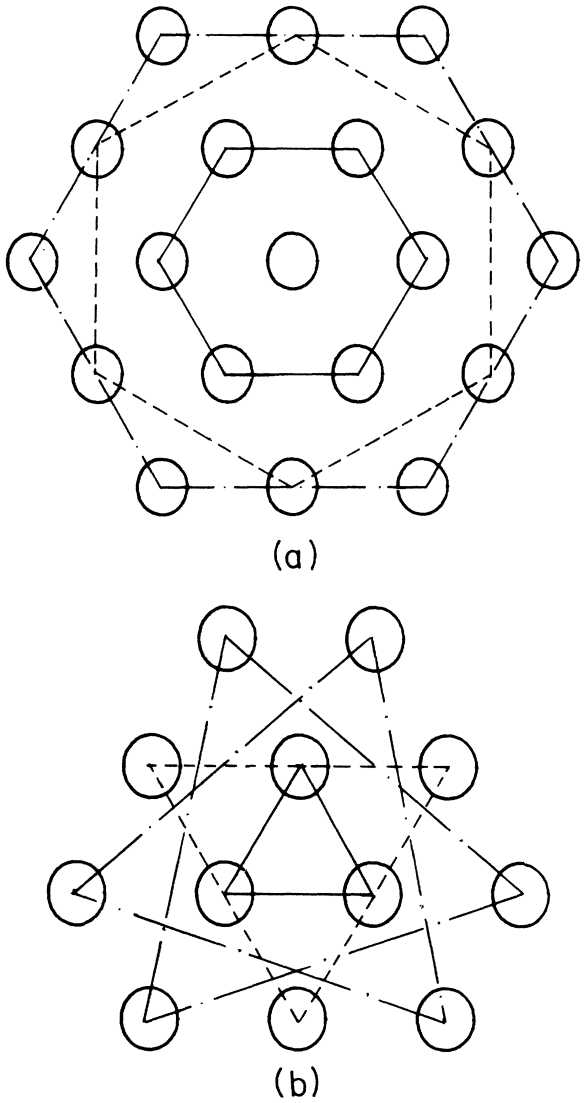

FIG. 4. Clusters used in calculation of many-adatom interactions. (a) For calculation of h_1, h_3, h_4, t_1, and t_3; (b) for calculation of h_2 and t_2.

the triangular interactions t_1 and t_3 (symmetry 3) as well as the hexagonal interactions h_1, h_3, and h_4 (symmetry 6). For the interactions t_2 and h_2 we used the 12-atom cluster, illustrated in Fig. 4(b) (symmetry 3). For the pair interactions, very little symmetry is present and both clusters were used.

III. RESULTS AND DISCUSSION

A. Site preference

Results for the difference in binding energy between the fcc and hcp sites are collected in Table I, for different distances of the adatom to the surface. d represents in fact the distance of the hydrogen atom from the jellium edge, i.e., the plane half-way between the surface and what would have been the next plane above the surface. We have indicated the relative contributions arising from the one-electron term δE^1 and the other term arising from the change in electron density at the adsite: $\delta E^2=\Delta E^0(\langle n_A\rangle)-\Delta E^0(\langle n_B\rangle)$. One notices that δE^2 is always negative. This is not surprising since the electron density at the fcc site is smaller than that at the hcp site. One also notices in general rather small values of δE^2, which have only a rather limited influence on the final result for $\Delta\epsilon$.

As regards δE^1, one notices in all cases very small variations with d. Large energy differences between the two sites are recorded in all but one case, namely, that of nickel where very small values of δE^1 were obtained. In most cases, the fcc site is more favorable to the hydrogen adatoms than the hcp site. One exception is that for H/Cu(111) where a preference for the hcp site is recorded. These results are in partial agreement with our own previously published results[41] where different clusters were used. In particular two distinct clusters were used for the calculation of the two binding energies at the different sites. The major differences between the two sets of results are for Cu and Pd where in our previous work, very small values of δE^1 were obtained.[41]

We thus find that in most cases there is a substantial preference of the hydrogen adatoms for one of the hollow sites (the fcc site for Ti, Co, Ru, Rh, and Pd and the hcp site for Cu), implying that for these metals it is very unlikely that any of the ordered structures requiring simultaneous occupation of the two types of hollow site [the (7×7) and (2×2) structures of Figs. 1(b) and 1(d)] will be formed. The one exception is for Ni, where basically no preference is shown for either type of site and thus one cannot, at this stage, discriminate between any of the ordered structures illustrated in Fig. 1.

The results for Ti(0001) are in excellent agreement with the results from other calculations,[18,42] where it was found that the fcc site is preferred to the hcp site by an energy of 0.2 eV.

B. Multiple-adatom interactions

We begin with a short description of the results for the quantities $\delta^{(n)}$ which represent the integrated change in density of states, with respect to E, when n interacting adatoms are introduced onto the metal cluster. Plotted in Fig. 5 is the particular case $\delta^{(6)}$ for six adatoms in the hexagonal ring arrangement: h_3 of Fig. 1(d) for the Ni(111) surface and for $d=0$. In the inset, we have also plotted the various components in the symmetry decomposition of $\delta^{(6)}$. Also plotted is the corresponding quantity for six noninteracting adatoms, i.e.,

$$\Delta(E)=\sum_{r=1}^{6}\delta_r(E)\ . \tag{11}$$

One notices that the hydrogen-induced resonance which is due to the coupling of the $1s$ orbital of the adatom with both the sp and d bands of the substrate is split into a series of resonances when the adatoms are allowed to interact with one another. Due to symmetry reasons, there are four of these resonances, two of which are doubly degenerate. Although quite substantial, this splitting is less pronounced than in cases where the adatoms are even closer together. One also notices quite important differences between $\delta^{(6)}$ and Δ in the region spanned by the Ni d bands and in particular in the lower part of the d band, indicating that d states from this energy region have a strong influence on the interadatom bonds.

In Fig. 6, the same quantities are plotted for the hexagonal ring arrangement h_2 of Fig. 1(f). Comparing the two sets of results one observes, first of all, a larger splitting of the hydrogen-induced resonance in the case of h_2 which is due to the closer proximity of the adatoms in this arrangement. One also observes in this case less marked differences between Δ and $\delta^{(6)}$ in the d-band region implying a less-pronounced participation of the d bands in the coupling between the adatoms. In order to better illustrate the differences between the two sets of results, we have plotted in Fig. 7(a) the difference curves $\delta^{(6)}-\Delta$ in both

TABLE I. Difference in binding energy: $\Delta\epsilon$ between the fcc and hcp hollow sites (in meV) for various values of d (in a.u.). Contributions to $\Delta\epsilon$ arising from one-electron term δE^1 and effective medium term δE^2 are given in parentheses as $(\delta E^1+\delta E^2)$.

d	0.0	0.1	0.2
Ti	−92 (−89−3)	−92 (−90−2)	−91 (−90−1)
Co	−49 (−33−16)	−45 (−31−14)	−42 (−30−12)
Ni	−13 (1−14)	−9 (3−12)	−7 (3−10)
Cu	50 (55−5)	51 (54−3)	52 (53−1)
Ru	−137 (−126−11)	−137 (−127−10)	−136 (−129−7)
Rh	−109 (−100−9)	−105 (−98−7)	−101 (−96−5)
Pd	−91 (91+0)	−88 (−88+0)	−86 (−86+0)

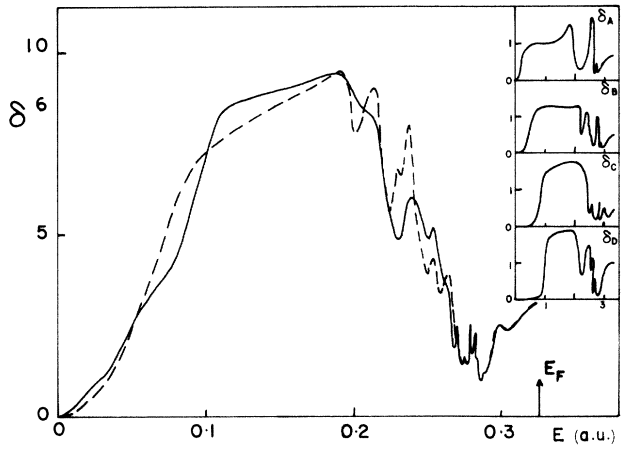

FIG. 5. Integrated change in density of states δ^6, arising when six interacting hydrogen adatoms, arranged in an h_3 configuration, are made to interact with the Ni cluster (solid curve) with corresponding quantity for six noninteracting H atoms (dashed curve). In the inset are represented the four different symmetry components of δ^6 [$\delta^6=\delta_A+2(\delta_B+\delta_C)+\delta_D$].

these cases.

In Fig. 7(b) we plot the corresponding quantities for the triangular rings in the arrangements of t_1, t_2, and t_3. As expected the largest splitting of the hydrogen-induced resonance is for the case where the adatoms are closest together (i.e., the t_1 configuration) and it decreases with increasing interadatom distance. On the other hand, one notices rather large disturbances in the d band for the t_3 configuration, indicating once more that the coupling between the hydrogen atoms in this configuration is strongly influenced by the Ni d states.

Let us now turn to the interaction energies. Collected in Table II are the values of $V^{(6)}$ for the hexagonal rings h_i ($i=1$–4) and $V^{(3)}$ for the triangular rings t_i ($i=1$–3), for H/Ni(111) and for different values of d. One notices very large repulsive interactions for the smallest hexagonal ring h_1, in which the adatoms are at

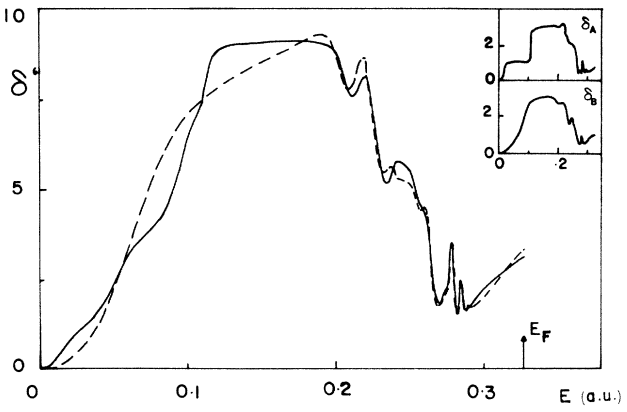

FIG. 6. Corresponding quantities for six H atoms arranged in an h_2 configuration ($\delta^6=\delta_A+2\delta_B$).

nearest-neighbor hollow sites on the surface. This is in agreement with experimental data which shows that the hydrogen saturation coverage on the Ni(111) surface is equal to 1 and thus far smaller than the value of 2 which occupation of all the threefold hollow sites would entail. This therefore reinforces our original assumption of nearest-neighbor exclusion in our description of the most plausible ordered overlayers which are likely to be formed on the substrate surface (see Fig. 1). As regards the h_2 ring, the interaction is small in magnitude and oscillates around 0 for varying values of d. The h_3 ring gives a pronounced attractive interaction (by far the most attractive of the four hexagonal rings), which is in accord with the LEED findings of Ref. 24. Finally, the h_4 ring gives rise to a very small attractive interaction. As far as the triangular rings are concerned, one notices a very attractive interaction for the t_3 configuration and small repulsive interactions for the other two configurations. It should be emphasized that a direct comparison of the two sets of results (for the hexagonal and triangular rings) is a little misleading, since, when taken over a whole layer, each hexagonal ring contributes two hydrogen adatoms, whereas each triangular ring contributes only half an adatom.

In order to interpret these results further, it proves useful to decompose the interaction energies into their con-

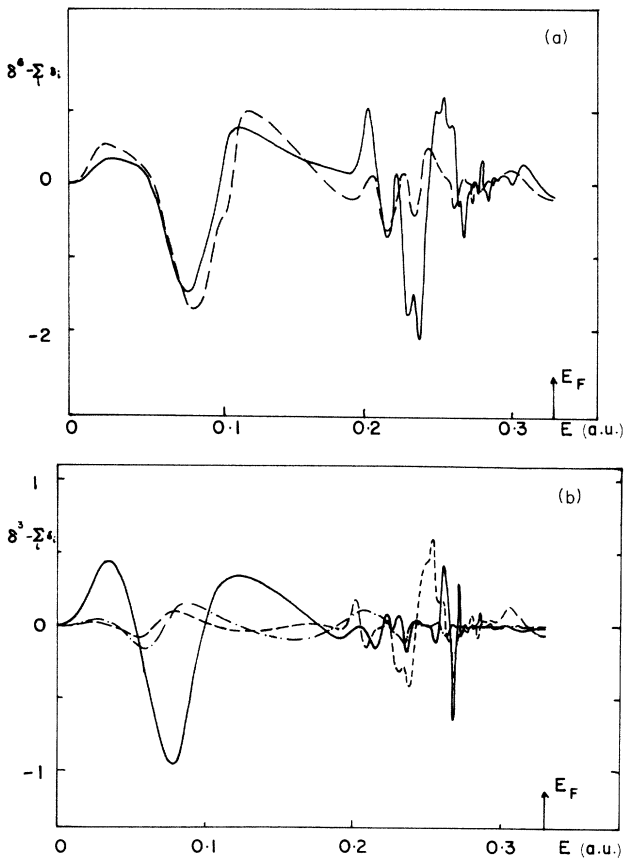

FIG. 7. (a) Difference curves: $\delta^6-\sum_i \delta_i$, for the cases illustrated in Fig. 5 (solid curve) and Fig. 6 (dashed curve). (b) Difference curves: $\delta^3-\sum_i \delta_i$, for the triangular ring arrangements t_1 (solid curve), t_2 (dash-dotted curve), and t_3 (dashed curve).

TABLE II. Multiple-adatom interactions (in meV) for six adatoms in hexagonal rings and three adatoms in triangular rings for H/Ni(111) for different values of d (in a.u.).

d	h_1	h_2	h_3	h_4	t_1	t_2	t_3
0	2164	−23	−153	−5	8	3	−53
0.1	1736	−3	−146	−4	13	2	−49
0.2	1187	12	−139	−4	17	2	−45

stituent pair interactions. We have calculated the pair interactions for two adatoms in up to sixth-nearest-neighbor hollow sites. Results for the H/Ni(111) system are collected in Table III. As a first and very important observation, we remark upon the excellent agreement which exists between the 3 (or 6) adatom interactions and the relevant sums of pairwise interactions (e.g., for the h_2 ring we take the sum of pair interactions corresponding to $6p_2+6p_5+3p_6$, etc.).

In fact all the information which has been obtained already by consideration of the hexagonal and triangular rings is contained in Table III. We notice very repulsive nearest-neighbor interactions (p_1) which are at the origin of the nearest-neighbor exclusion, strongly attractive sixth-neighbor interactions (p_6) which are at the origin of the formation of the ordered structures of (2×2) symmetry, fairly attractive third-neighbor interactions (p_3) which stabilize the graphitic (2×2) overlayer, slightly repulsive second-neighbor interactions (p_2) which act against the ordered structure of (1×1) symmetry and negligible fourth- and fifth-neighbor interactions which eliminate the possibility of formation of structures of $(\sqrt{3}\times\sqrt{3})$ and (7×7) symmetry.

A consideration of the pairwise interactions therefore gives us all the information required to arrive at general conclusions regarding the formation (or not) of ordered hydrogen overlayers on metal surfaces.

The lattice-gas Hamiltonian [Eq. (1)] can thus be simplified to take account of only the pairwise interactions:

$$H-\mu N=-\epsilon_0\sum_i n_j-\sum_{i\neq j}v_{ij}n_in_j-\Delta\epsilon\sum_i{}' n_i \qquad (12)$$

and $\epsilon_0=\epsilon+\mu$. The ground-state energies of each of the ordered structures illustrated in Fig. 1 can be obtained quite simply and we find

$$U_A=-(\epsilon_0+3p_6)/8\ ,$$

$$U_B=-(2\epsilon_0+6p_4-\Delta\epsilon)/14\ ,$$

$$U_C=-(\epsilon_0+3p_5)/6\ ,$$

$$U_D=-(2\epsilon_0+3p_3+6p_6-\Delta\epsilon)/8\ ,$$

$$U_E=-(\epsilon_0+p_2+p_5+3p_6)/4\ ,$$

$$U_F=-\epsilon_0/3-(p_2+2p_5+p_6)/2\ ,$$

$$U_G=-3(\epsilon_0+2p_2+2p_5+3p_6)/8\ ,$$

$$U_H=-(\epsilon_0+3p_2+3p_5+3p_6)/2\ .$$

If one uses the p values of Table III and the $\Delta\epsilon$ values of Table I one finds that the (2×2) graphitic structure is the most stable over a wide range of ϵ_0. The only effect which might change this state of affairs would be the introduction of a fairly repulsive $\Delta\epsilon$ which would act against the honeycomb (2×2) structure [see Fig. 1(a)] and in favor of the triangular (2×2) structure of Fig. 1(a), the rectangular (2×1) structure of Fig. 1(e), and the Kagomé (2×2) structure of Fig. 1(g).

The experimental results of Christmann *et al.* showed the presence of an ordered structure of (2×2) symmetry over a wide range of coverages between $\Theta\approx0.2$ and 0.6.[24] Theoretical derivations of the phase diagram of the transition temperature versus hydrogen coverage, using a renormalization-group calculation,[43] have shown that, for a model with nearest-neighbor exclusion ($p_1=+\infty$), second-neighbor repulsion ($p_2>0$), and no further neighbor interactions ($p_i=0$, $i>2$), the range of hydrogen coverages is far narrower than in the experimental case ($0.45<\theta<0.52$). A more recent calculation,[44] also using renormalization-group theory, but including up to sixth-neighbor interactions, shows a much wider range of hydrogen coverages where the (2×2) structure may be formed. Long-range interactions are thus of great importance in the description of the experimental phase diagram, as they are also seen to be in the present work.

We now consider other systems specifically. We start with the case of H/Ti(0001). We recall first of all that a pronounced preference for the fcc site was recorded (see Table I) and this will act against the formation of the honeycomb structures of (7×7) and (2×2) symmetry [see Figs. 1(b) and 1(d)]. The pair interactions for different values of d are given in Table IV. If one uses these values in the expressions for the ground-state energies, one finds that the (1×1) structure [see Fig. 1(h)] is the most stable of those illustrated in Fig. 1, for all values of ϵ_0.

We now consider H/Co(0001). The results for the pair

TABLE III. Pair interactions (in meV) for H/Ni(111) for different values of d (in a.u.).

d	p_1	p_2	p_3	p_4	p_5	p_6
0	400	2	−6	1	1	−18
0.1	310	4	−5	1	1	−17
0.2	220	6	−5	1	1	−15

TABLE IV. Pair interactions for H/Ti(0001).

d	p_2	p_3	p_4	p_5	p_6
0	−8	−30	−13	−8	0
0.1	−8	−27	−11	−8	0
0.2	−8	−26	−10	−8	0

TABLE V. Pair interactions for H/Co(0001).

d	p_2	p_3	p_4	p_5	p_6
0	3	−1	−1	0	−18
0.1	5	0	−1	0	−17
0.2	6	−1	−2	0	−15

TABLE VII. Pair interactions for H/Ru(0001).

d	p_2	p_3	p_4	p_5	p_6
0	0	7	−2	0	−13
0.1	0	7	−2	0	−13
0.2	0	6	−2	0	−13

interactions are collected in Table V. These are very similar to those for H/Ni(111) (see Table III). The main difference between the two chemisorption systems are with respect to the $\Delta\epsilon$ values. Whereas for Ni typical values were small (i.e., <10 meV), for Co, $\Delta\epsilon$ is found to be about five times larger. This has important consequences with respect to which structures are formed on the surface. The graphitic (2×2) structure is no longer the most stable, and one finds from the ground-state energies that for different values of ϵ_0 (i.e., for different coverages), the triangular (2×2), the rectangular (2×1) and the Kagomé (2×2) structures may be formed, before the saturated (1×1) structure is formed.

For H/Cu(111), one finds again a fairly large value of $\Delta\epsilon$, but this time the preference is for the hcp site. The pair interactions for this system are collected in Table VI; one finds that these are generally small, indicating perhaps a tendency for none of the ordered structures illustrated in Fig. 1 to be formed. Substituting these values in the expressions for the ground-state energies, one finds that the two structures of $(\sqrt{3}\times\sqrt{3})$ are marginally more stable than any of the other structures.

We now consider H/Ru(0001). The binding-energy difference between the fcc and hcp sites is the largest one found for the seven metals studied here. The pair interactions are tabulated in Table VII. Substitution of the p_i values in the expressions for the ground-state energies shows that the (1×1) structure [see Fig. 1(h)] is the most stable for all values of ϵ_0.

For H/Rh(111), the situation is reminiscent to that found for H/Co(0001). The results for the pair interactions are collected in Table VIII. The repulsive $\Delta\epsilon$ acts against the graphitic (7×7) and (2×2) structures. The large attractive p_6 favors the structures of (2×2) and (2×1) symmetry. The repulsive p_2 ensures that the (1×1) structure is not formed over all H coverages. Substituting for the p values in the expressions for the ground-state energies shows that the triangular $p(2\times2)$, the rectangular (2×1), and the Kagomé (2×2) structures are at different hydrogen coverages the most stable of the structures illustrated in Fig. 1.

Finally, let us consider the case of hydrogen on palladium. This system has been the object of a number of recent investigations. The LEED study of Felter and Stulen shows the presence of two ordered superstructures of $(\sqrt{3}\times\sqrt{3})$ symmetry which they attribute to the formation of the ordered overlayers depicted in Figs. 1(c) and 1(f).[25] The embedded-atom calculation of Foiles and Daw[45] show that the structure of $(\sqrt{3}\times\sqrt{3})$ symmetry have indeed lowest energy, especially if the hydrogen atoms are made to occupy subsurface octahedral sites. The notion that hydrogen atoms penetrate below the surface has also been advanced by Chan and Louie[46] in their attempts to interpret the ARUPS results of Ref. 3. In these experiments, a marked difference between the spectra recorded at low temperatures and those taken at room temperature was observed. At low temperatures ($T<150$ K) the spectra showed the presence of a hydrogen-induced state located below the metal d bands and a rearrangement of states within the d band. At room temperature, the spectra were more reminiscent of those obtained for the clean Pd(111) surface, although the presence of the hydrogen atoms was detected at or near the surface. Chan and Louie's interpretation of these results is that at low temperatures, the hydrogen atoms adsorb above the surface in the threefold hollow sites and form an ordered (1×1) layer, whereas at higher temperatures the hydrogen atoms penetrate below the surface and occupy subsurface octahedral sites, in which case the calculations show that the hydrogen-induced state has no d character. On the other hand, Chubb and Davenport[47] give a different interpretation of the photoemission results. In this work, they attribute the differences in the photoemission spectra to a decrease in hydrogen coverage as the temperature is raised. Our own tentative interpretation[30] is that the hydrogen atoms may occupy different sites on the surface, and that considerable mobility of the H atoms may be expected.

Assuming that the hydrogen atoms are adsorbed in the threefold hollow sites, we have calculated the difference $\Delta\epsilon$ in binding energy between the fcc and hcp sites, which is given in Table I, as well as the pair interactions which are tabulated in Table IX. The large value of $\Delta\epsilon$ rules out the two graphitic structures of (7×7) and (2×2) symmetry [see Figs. 1(b) and 1(d)]. The only fairly attractive interaction is p_6, while p_2 is repulsive and p_3, p_4, and p_5 are practically zero. Substitution of these results in the expression for the ground-state energies shows that the

TABLE VI. Pair interactions for H/Cu(111).

d	p_2	p_3	p_4	p_5	p_6
0	−2	0	0	−2	1
0.1	3	−2	0	−1	3
0.2	8	−4	0	−1	2

TABLE VIII. Pair interactions for H/Rh(111).

d	p_2	p_3	p_4	p_5	p_6
0	7	5	−1	0	−21
0.1	6	2	−1	−1	−21
0.2	7	3	−1	0	−20

TABLE IX. Pair interactions for H/Pd(111).

d	p_2	p_3	p_4	p_5	p_6
0	10	−1	0	0	−10
0.1	11	0	0	0	−10
0.2	12	1	0	0	−9

structures of (2×2) symmetry are more stable than any of the others and one would expect that at different values of ϵ_0, the triangular (2×2), the rectangular (2×1), and the Kagomé (2×2) structures may be formed. These results are in disagreement with the LEED data of Ref. 25. The very small values recorded for p_5 and the comparatively much larger values of p_6 are responsible for our conclusions. We have also calculated many adatom interactions in the hope that the many-body contributions might correct the trend, but these corrections proved to be extremely small and exerted no influence on the final ordering of the different structures. The present model, which showed remarkable agreement with experiment for H/Ni(111), falls short of agreement with the experimental findings for H/Pd(111).

In trying to determine the reasons for this discrepancy, we have looked at various possibilities which might have an influence on the results. We have looked at the possibility that the hydrogen atoms are not adsorbed in the threefold hollow sites above the surface. In particular, we have looked at the possibility that the H atoms are located in bridge sites, which proved to be rather attractive to the H atoms.[30] The lattice which is available for occupation by the hydrogen atoms is a Kagomé lattice instead of the honeycomb lattice encountered for center-site adsorption. The situation in this case is rather more complex than that experienced for the honeycomb lattice and we have by no means considered all the possible ordered overlayer configurations which may arise on that lattice. Nevertheless, we did look at the structures of $(\sqrt{3}\times\sqrt{3})$ symmetry and found these not to be in any way more attractive than other structures. We have also considered the possibility that subsurface sites are occupied, but found that these sites were considerably more repulsive to the hydrogen atoms than were surface sites.

Finally, we considered the possibility of a uniform relaxation of the surface. Some changes in the calculated values of the different p's were recorded. In particular, it was found that a uniform contraction of the surface plane resulted in a reduction of the attractive interaction p_6 and a reduction of the repulsive interaction p_2, with very little change in the values of the other interactions. The gradual decrease in p_6 makes it more difficult for the structures of (2×2) and (2×1) symmetry to be formed, however the lack of any attractive p_5 would still act against the formation of structures of $(\sqrt{3}\times\sqrt{3})$ symmetry. An outward relaxation of the surface results in the opposite effect, namely, p_6 becomes more attractive and thus the structures of (2×2) and (2×1) symmetry are even more stable than in the unrelaxed case. Finally, we note that the magnitude of this effect is rather small and one would need a substantial contraction ($>10\%$) of the surface plane in order for the values of p_5 and p_6 to become comparable. Such a large contraction would seem rather unrealistic in the case of a close-packed surface of a transition metal. We must thus rule out relaxation of the surface as a possible explanation of the discrepancy between our results and the experimental data.

Other possible reasons for the discrepancy include the inadequacies of the present model, amongst which we note the fact that bulk band structure muffin-tin potentials were used to describe the metal atoms,[35] while the clusters of metal atoms included surface atoms only.

IV. CONCLUSION

We have presented a model for the calculation of interaction energies between H adatoms on the close-packed surface of fcc and hcp transition and noble metals. Assuming that the H adatoms occupy threefold hollow sites, then the important parameters regulating the formation of ordered overlayers on the surface are the difference in binding energy $\Delta\epsilon$ between the fcc and hcp hollow sites and the various interaction energies between the adatoms. The values of $\Delta\epsilon$ were found to be fairly large for most of the metals studied here and could thus not be neglected in the description of the stability of the various ordered structures. This meant that ordered overlayers requiring the simultaneous occupation of both types of hollow sites were found to be rather unstable. The exception was for H/Ni(111) where very small values of $\Delta\epsilon$ were recorded and where the most stable structure was a honeycomb structure in which both types of hollow sites were occupied.

Calculation of multiple-adatom interactions showed that these may be written, to a high degree of accuracy, as the relevant sum of pair interactions, thereby indicating that multiple-adatom effects are small and should not play an important role in the description of the stability of the overlayers. Nearest-neighbor interactions were found to be very repulsive in all cases, indicating that only ordered structures with nearest-neighbor exclusion could be formed. Long-range interactions were found to be nonnegligible, especially in the case of the sixth-neighbor interaction, which proved to be at the origin of the greater stability of a number of ordered overlayers with (2×2) symmetry.

The stability of the most plausible ordered overlayers on a honeycomb lattice was analyzed through comparison of the ground-state energies of the various structures. Comparison with experiment was made whenever possible. Excellent agreement with the experimental data for H/Ni(111) was obtained, but major discrepancies with the data for H/Pd(111) were also found.

ACKNOWLEDGMENT

I would like to acknowledge the financial support of the Swiss National Science Foundation, through Grant No. 2847-083.

[1]K. Christmann, Surf. Sci. Rep. (to be published).
[2]I. Toyoshima and G. A. Somorjai, Catal. Rev. Sci. Eng. **19**, 105 (1979).
[3]W. Eberhardt, F. Greuter, and E. W. Plummer, Phys. Rev. Lett. **46**, 1085 (1981).
[4]M. A. van Hove and S. Y. Tong, in *Surface Crytallography by LEED*, edited by R. Gomer (Springer-Verlag, Berlin, 1979).
[5]M. Weinert and J. W. Davenport, Phys. Rev. Lett. **54**, 1547 (1985).
[6]C. Umrigar and J. W. Wilkins, Phys. Rev. Lett. **54**, 1551 (1985).
[7]S. G. Louie, Phys. Rev. Lett. **42**, 476 (1979).
[8]T. H. Upton and W. A. Goddard, Phys. Rev. Lett. **42**, 472 (1979).
[9]J. K. Nørskov, Phys. Rev. Lett. **48**, 1620 (1982); P. Nordlander, S. Holloway, and J. K. Nørskov, Surf. Sci. **136**, 59 (1984).
[10]T. L. Einstein, in *Chemistry and Physics of Solid Surfaces*, edited by R. Vanselow and R. Howe (Springer-Verlag, Berlin, 1982), Vol. IV, p. 251.
[11]T. B. Grimley, Proc. Phys. Soc. London Sect. B **90**, 751 (1967); T. B. Grimley and S. M. Walker, Surf. Sci. **14**, 395 (1969).
[12]T. L. Einstein and J. R. Schrieffer, Phys. Rev. B **7**, 3629 (1973); T. L. Einstein, CRC Crit. Rev. Solid State Mater. Sci. **7**, 260 (1978).
[13]K. H. Lau and W. Kohn, Surf. Sci. **75**, 69 (1978).
[14]K. Schönhammer, V. Hartung, and W. Brenig, Z. Phys. B **22**, 143 (1975).
[15]N. Burke, Surf. Sci. **58**, 349 (1976).
[16]K. Masuda, J. Phys. (Paris) **40**, 299 (1979).
[17]J. K. Anderson, in *Structure of Metallic Catalysts* (Academic, New York, 1975).
[18]P. J. Feibelman, D. R. Hamann, and F. J. Himpsel, Phys. Rev. B **22**, 1754 (1980).
[19]F. Greuter, W. Eberhardt, and E. W. Plummer (unpublished).
[20]P. Hofmann and D. Menzel, Surf. Sci. **152/153**, 382 (1985).
[21]W. Eberhardt, S. G. Louie, and E. W. Plummer, Phys. Rev. B **28**, 465 (1983).
[22]F. Greuter and E. W. Plummer, Solid State Commun. **48**, 37 (1983).
[23]G. Casalone, M. G. Cattania, M. Simonetta, and M. Tescari, Surf. Sci. **72**, 739 (1978).
[24]K. Christmann, R. J. Behm, G. Ertl, M. A. van Hove, and W. H. Weinberg, J. Chem. Phys. **70**, 4168 (1979).
[25]T. E. Felter and R. H. Stulen, J. Vac. Sci. Technol. A **3**, 1566 (1985).
[26]J. T. Yates, P. A. Thiel, and W. H. Weinberg, Surf. Sci. **84**, 427 (1979).
[27]L. R. Danielson, M. J. Dresser, E. E. Donaldson, and J. T. Dickinson, Surf. Sci. **71**, 599 (1978).
[28]K. Christmann, G. Ertl, and T. Pignet, Surf. Sci. **54**, 365 (1976).
[29]M. J. Puska, R. M. Nieminen, M. Manninen, B. Chakraborty, S. Holloway, and J. K. Nørskov, Phys. Rev. Lett. **51**, 1081 (1983).
[30]J. P. Muscat, Surf. Sci. **148**, 237 (1984).
[31]P. K. Johansson, Solid State Commun. **31**, 591 (1979).
[32]J. P. Muscat, Surf. Sci. **110**, 85 (1981).
[33]J. P. Muscat, Prog. Surf. Sci. **18**, 59 (1985).
[34]J. P. Muscat, Surf. Sci. **152/153**, 684 (1985).
[35]V. L. Moruzzi, J. F. Janak, and A. R. Williams, *Calculated Electronic Properties of Metals* (Pergamon, New York, 1978).
[36]C. O. Almbladh, U. von Barth, Z. D. Popovic, and M. J. Stott, Phys. Rev. B **14**, 2250 (1976).
[37]M. E. Rose, *Elementary Theory of Angular Momentum* (Wiley, New York, 1957).
[38]J. K. Nørskov, Phys. Rev. B **26**, 2875 (1982).
[39]E. Clementi and C. Roetti, At. Data Nucl. Data Tables **14**, 177 (1984).
[40]P. Nordlander and S. Holmström (private communication).
[41]J. P. Muscat, Surf. Sci. **110**, 389 (1981).
[42]P. Cremaschi and J. L. Whitten, Surf. Sci. **112**, 343 (1981).
[43]E. Domany, M. Schick, and J. S. Walker, Solid State Commun. **30**, 331 (1979).
[44]K. Nagai, Y. Ohno, and T. Nakamura, Phys. Rev. B **30**, 1461 (1984).
[45]S. M. Foiles and M. S. Daw, J. Vac. Sci. Technol. A **3**, 1565 (1985).
[46]C. T. Chan and S. G. Louie, Phys. Rev. B **30**, 4153 (1984).
[47]S. R. Chubb and J. W. Davenport, Phys. Rev. B **31**, 3278 (1985).